Electrochemical Materials and Technologies

ARTICLE

Electrochemical Materials and Technologies

eISSN: 2949-0561

Cite this: Electrochem. Mater. Technol. 3 (2024) 20243027

Stability and reproducibility of the amperometric sensors for oxygen concentration analysis in the nitrogen gas mixtures

Anatoly Kalyakin [a], Alexander Volkov [a *], Daria Mirzayants [a]

Received: 26 December 2023
Accepted: 4 March 2024
Published online: 12 March 2024

DOI: 10.15826/elmattech.2024.3.027

The paper presents experimentally obtained results on the long-term stability tests of the solid electrolyte amperometric sensor output signal during the operation in the $O_2 + N_2$ gas mixtures. These data prove the stability and reproducibility of the output signal when measuring the oxygen concentration in air for 8000 hours. The output signal variation during the tests did not exceed ± 2 %. We performed four heating / cooling cycles of different durations, which did not influence either sensor integrity or operation characteristics. The structure of the solid electrolyte sensor and the solid electrolyte/electrode interfacial layer remained unchanged during the tests. Dynamic characteristics of the sensor, including the response time, were stable.

keywords: solid electrolyte, sensor, stability, limiting current, response time

1. Introduction

Solid electrolytes with oxygen-ionic conductivity are widely used in sensors aimed at the analysis of free oxygen concentration in gaseous media and in metallic melts [1–9]. There is a vast number of published works on the development of potentiometric solid electrolyte sensors with the mixed potential based on oxygen-conducting solid electrolytes with unseparated gas areas, which are used to measure the concentration of different gases in air [10–15]. In such sensors when detecting the analyzed gas, for instance, hydrogen in air or oxygen-containing media, the processes resulting in the deviation of the concentration dependence from the Nernstian one are observed. Such behavior may be caused by the simultaneous occurrence of potential-determining processes, accumulation of the process product or slowed adsorption at the three-phase boundary. However, these deviations are most likely caused by the processes that proceed simultaneously at the sensor measuring electrode:

$$^1/_2\, O_2 + 2e^- = O^{2-}, \quad (1)$$

$$Red + O^{2-} = Ox + 2e^-, \quad (2)$$

where Ox = CO_2 or H_2O; Red = CO or H_2.

For such sensors the dependence of the generated electro motive force (EMF) on the concentration of the combustible component in the analyzed gas is described by Equation (3):

$$E = E_0 + k \cdot \ln[H_2], \quad (3)$$

where k is an empirically fitted constant.

Simultaneous Reactions (1) and (2) are the main reasons for the so-called Nernstian or mixed potential.

a: Institute of High-Temperature Electrochemistry of the Ural Branch of the Russian Academy of Sciences, Ekaterinburg 620066, Russian Federation

* Corresponding author: a.volkov@ihte.ru

The difference in the mixed potential from the equilibrium oxygen potential becomes greater when the difference between the rates of Reactions (1) and (2) increases. In addition, the value of the appeared mixed potential is determined mainly by the composition and concentration of the analyzed combustible component, materials of the measuring electrode and operation temperature.

Potentiometric oxygen sensors based on the YSZ solid electrolytes are the most widely used. These sensors on solid electrolytes with unipolar oxygen conductivity proved themselves to be highly efficient in heat engineering, metallurgy, chemistry, and motor industry. These sensors are characterized by wide oxygen concentration measuring range, high operation rate, simplicity of construction and simple recalculation of the obtained electrical signal (EMF) into the oxygen concentration value. However, despite the above mentioned advantages of such sensors, the reference gas with known and stable oxygen concentration required for the sensor operation is a significant drawback, as in some cases the reference gas supply can hardly be provided and, therefore, the sensor operation becomes more complicated [16–22].

The increased number of published materials on solid electrolyte amperometric sensors with diffusion barriers aimed at the analysis of oxygen, hydrogen and moisture concentrations in inert and oxidized gas media have recently appeared [23–29]. The sensor designs, perspective solid electrolytes compositions, electrode materials, optimal operating temperatures for the analysis, etc. have been suggested [30–35]. As opposed to the potentiometric sensors, amperometric sensors on solid electrolytes have a significant advantage, i.e. they do not need any reference gas. This allows using them under the conditions when oxygen or any other gas supply to the sensor is hindered. Nevertheless, basic operation conditions (calculation scale, reaction rate, accuracy, simplicity of construction and operation, ability to analyze oxygen micro concentration) make the potentiometric sensors indispensable.

In view of the growing interest towards the amperometric sensors with diffusion barriers, we evaluated the long-term stability of the sensor output signal during 8000 hours, as well as the reproducibility of the measurement results and response time. The structures of the sensor solid electrolyte and electrodes during the tests were analyzed.

2. Experimental

2.1. Samples preparation

The present paper reports on the analysis of the sensor, i.e., an electrochemical cell, based on the oxygen-conducting solid electrolyte of the $0.9ZrO_2 + 0.1Y_2O_3$ composition. The plates of the solid electrolyte were produced at the Chepetsky Mechanical Plant JSC (Glazov, Russia). The schematic of the sensor is presented in Figure 1 and its appearance is provided in Figure 2. The sensor was made of two solid electrolyte plates with the length of 25 mm, width of 12 mm, and thickness of 1 mm. One of the plates had a cavity of 0.5 mm and a diameter of 6 mm. Porous Pt electrodes of 1 mm thickness were applied to the opposite sides of the solid electrolyte concave plate by the method of screen printing. The current leads were made of 0.1 mm Pt wire and located together with the Pt electrodes. A ceramic capillary of the 267 μm inner diameter and 20 mm length was located between the electrolyte plates. The plates were glued with the heat resistant glass. To apply the constant current voltage on the electrochemical cell a GPS-18500 constant current source ("MORNSUN" Company, China) was used; the value of the current that passed through the cell was measured by a GDM-8246 type multimeter ("Good Will Instrument" Company, Taiwan). Cylinder-stored compressed air was used as an analyzed gas and $O_2 + N_2$ gas mixtures containing 0.5, 2, 12 and 16 % of oxygen were used as calibration gases.

A constant current voltage was applied to the sensor electrodes with the polarity that enabled the oxygen pumping out from the inner sensor cavity to the flow of the analyzed gas. The exchange between input air to the cavity and output nitrogen from the cavity proceeded via the capillary. When a definite value of the applied voltage was reached these processes equilibrated and the limiting current appeared.

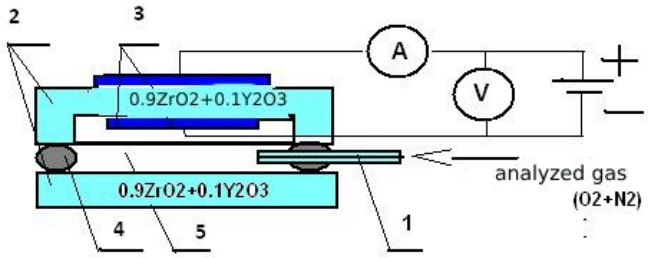

Figure 1 Schematic of the amperometric cell: 1 – capillary, 2 – solid electrolyte plates, 3 – outer and inner electrodes, 4 – glass sealant, 5 – cavity. A denotes amperemeter, V denotes voltmeter.

Figure 2 Photograph of the sensor after 8000 hours tests.

The value of the limiting current according to Equation (4) is used to calculate the oxygen concentration in the analyzed gas.

$$I_{limiting} = \left(\frac{4F \cdot P \cdot D_{O_2} \cdot S}{R \cdot T \cdot L}\right) \cdot \ln\left(1 - C_{O_2}\right), \quad (4)$$

where $4F$ is the amount of electricity required to transfer one mole of oxygen; P is the total pressure of the analyzed gas; D is the oxygen diffusion coefficient in nitrogen [36]; S and L denote the cross section and length of the capillary diffusion channel; R is the gas constant; T is the absolute temperature; C_{O_2} is the oxygen concentration, expressed in volume fractions. This is true for a common molecular diffusion of the gas via a capillary, as it is in our case. The diffusion coefficient depends on the temperature and pressure as follows:

$$D = D_0 \cdot \left(\frac{T}{273}\right)^{\partial} \cdot \frac{1}{P}, \quad (5)$$

where D_0 is a standard value of the diffusion coefficient at 0 °C. When plugging Equation (5) into Equation (4) it is seen that for a common molecular diffusion, the limiting current of the sensor does not depend on the gas pressure and it is proportional to $T^{\acute{\alpha}-1}$.

2.2. Experiment procedures

The sensor presented in Figure 1 was placed into the tubular furnace with a nichrome heater. The volume of the tubular furnace was 0.65 l. The temperature in the furnace was maintained with the accuracy of ± 3 °C using the TP 703 Varta regulator ("NPK Varta" Ltd, Saints-Petersburg, Russia). The analyzed gas mixture was flown through the inner chamber of the furnace with the flow rate of 20 ml/min. The gas mixture of the desired composition was obtained by additional purification of the cylinder-stored air from moisture and admixtures (ciolite). The sampling was performed using the gas consumption regulators of the F-201C-33-V type ("SONSTIGES" Company, Denmark). The sensor operated in a pulse regime, i.e. during the whole operation period there were 4 heating-cooling cycles to check the sensor thermal resistance. The duration of heating-cooling cycles varied from several hours to several days.

3. Results and discussion

When the sensor was heated up to the temperature of 700 °C the constant current voltage was applied to the electrodes. As the applied voltage grew; the current passing through the sensor solid electrolyte plate started growing. When a definite value of the applied voltage was reached the current reached a definite value and stabilized. This stabilized value is a limiting current. For each oxygen concentration in the analyzed gas mixture the limiting current values are constant under otherwise equal conditions (parameters of diffusion barrier, temperature, gas mixture composition and pressure). Figure 3 illustrates voltammetry characteristics of the sensor during the oxygen content determination in air at the temperature of 700 °C.

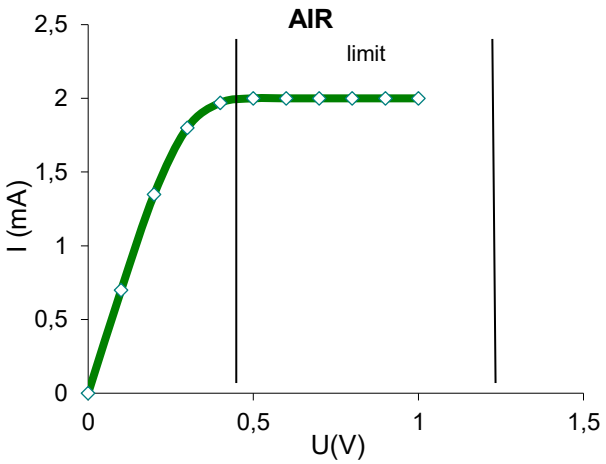

Figure 3 Dependence of the sensor current on the applied voltage.

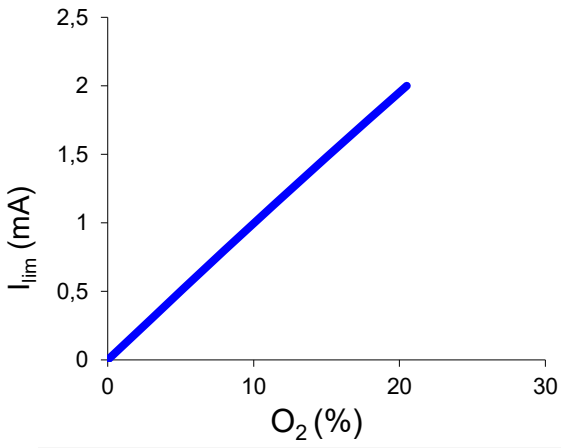

Figure 4 Dependence of the sensor limiting current on the oxygen concentration.

The limiting current is seen to appear only at the voltage of 0.4 V. Determination of the sensor limiting currents for gaseous mixtures containing from 0 to 20.5 % of oxygen allowed obtaining the linear dependence of limiting currents on the oxygen concentration, illustrated in Figure 4.

Apart from the sensor characteristics, illustrated in Figures 3 and 4, we recorded the dynamic characteristics of the sensor before long-term stability tests (Figures 5, 6 and 7). We determined the time intervals for the beginning of the sensor operation and the actual sensor signal of 90 % of the nominal value. Time required for the first response was 3–5 seconds and time required for the sensor signal operation at 90 % of the nominal value varied from 20 to 60 seconds (these values were obtained using the transport delay, i.e. the time required for a gas flow to move from the gas cylinder reducer to the sensor). The time range of 40 sec of the sensor response needed to reach 90 % of the nominal value may be explained by the fact that dynamic characteristics differ both at the significant increase and decrease in the oxygen concentration.

The dynamic characteristics of the sensor were verified after 4000 hours of operation and 8000 hours (Figures 6 and 7, respectively).

Figures 5, 6 and 7 illustrate that the dynamic characteristics of the sensor remained stable during the long-term endurance tests. The sensor proved to have good reproducibility of the results. Deviations of the limiting current values during the tests were ± 2 % form the average value.

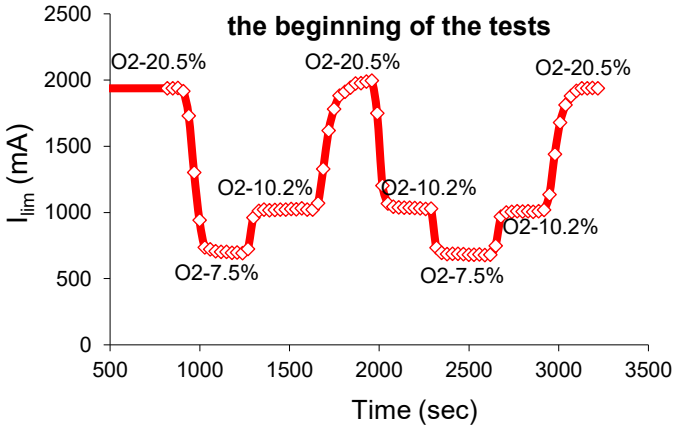

Figure 5 Dynamic characteristics of the sensor on the oxygen concentrations changes at the beginning of the tests.

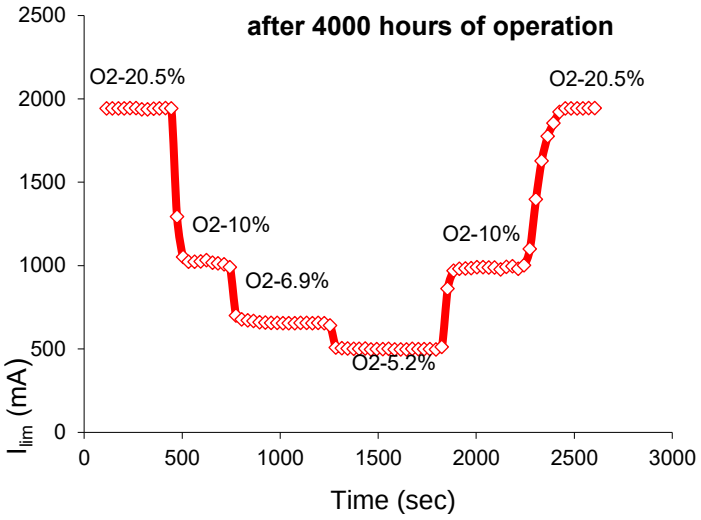

Figure 6 Dynamic characteristics of the sensor on the oxygen concentration changes after 4000 hours of operation.

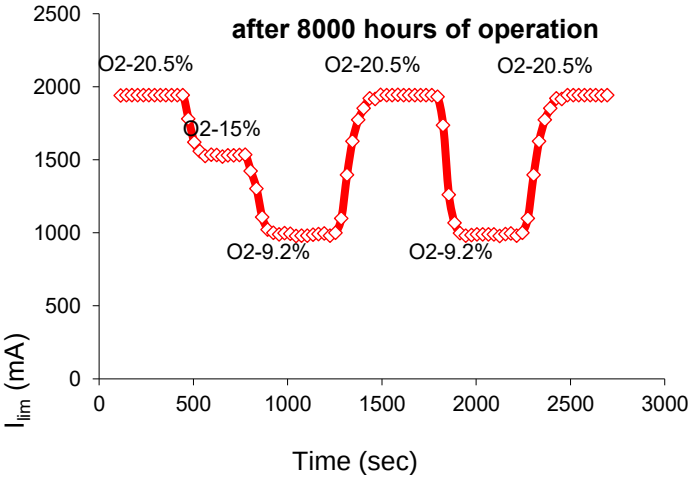

Figure 7 Dynamic characteristics of the sensor on the oxygen concentration changes after 8000 hours of operation.

Figure 8 illustrates the dependence of the sensor limiting current changes at oxygen content determination in air for 8000 hours. There were four heating-cooling cycles of different time. The abrupt temperature variations did not cause any destruction or depressurization of the sensor.

Figure 9 presents SEM images of the sensor electrode / electrolyte interface before and after the tests. It is seen that the structure of the solid electrolyte sensor and the interfacial layer of the solid electrolyte / electrode during the tests remained unchanged.

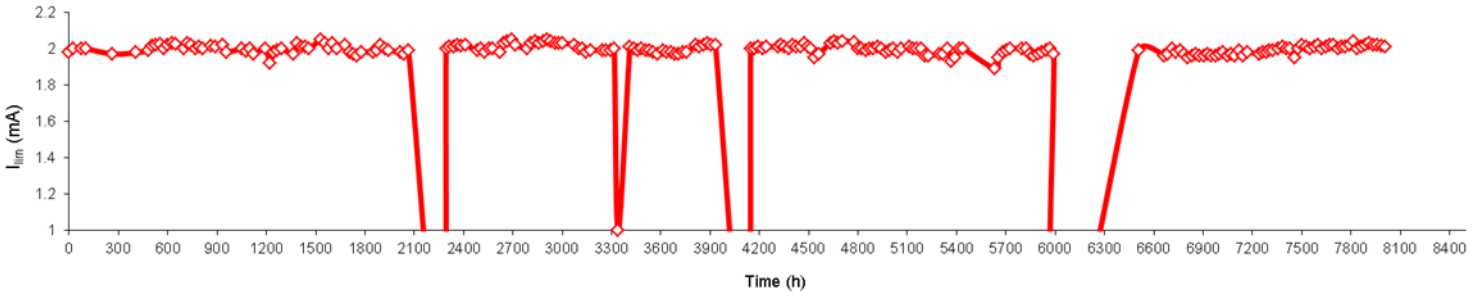

Figure 8 Changes in the sensor limiting current during the operation.

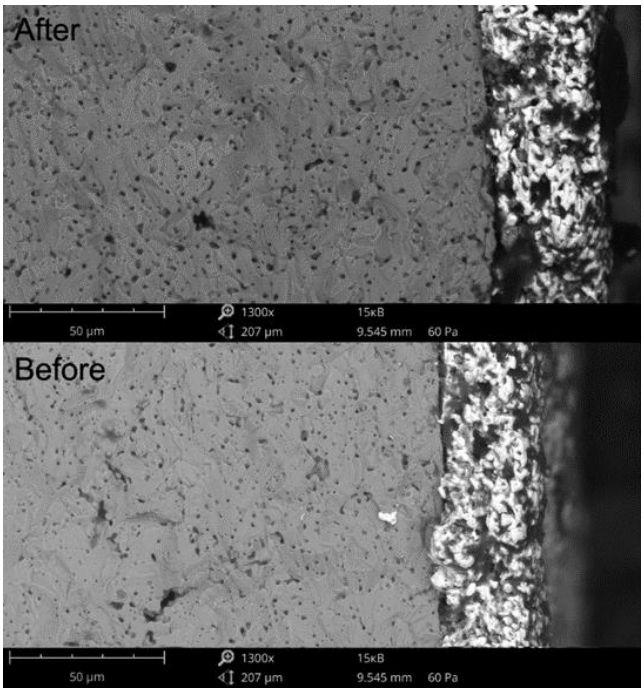

Figure 9 SEM-images of the sensor electrode / electrolyte interface before and after the tests.

4. Conclusions

The stability of the amperometric sensor based on the YSZ solid electrolyte with diffusion barrier was studied when measuring oxygen concentration in air for 8000 hours. The sensor demonstrated stable operation and stable reproducibility of results. The performed heating-cooling cycles did not result in the sensor operation failure. This sensor may be considered promising for implementation.

Supplementary materials

No supplementary materials are available.

Funding

The present research was performed within the budget plan of the Institute of High Temperature Electrochemistry.

Acknowledgments

None.

Author contributions

Anatoly Kalyakin: Data curation; Formal Analysis; Investigation; Methodology.

Alexander Volkov: Investigation; Validation; Data curation; Methodology; Resources; Supervision; Writing – Original draft; Writing – Review & Editing.

Daria Mirzayants: Writing – Review & Editing; Visualization.

Conflict of interest

The authors declare no conflicts of interest.

Additional information

Anatoly Kalyakin, https://orcid.org/0000-0002-8816-4303;

Alexander Volkov, https://orcid.org/0000-0002-5184-986X.

References

1. Okamoto H, Obayashi H, Kudo T, Carbon monoxide gas sensor made of stabilized zirconia, Solid State Ion., **1(3–4)** (1980) 319–326. https://doi.org/10.1016/0167-2738(80)90012-0

2. Sorita R, Kawano T, A highly selective CO sensor: screening of electrode materials, Sens. Actuator. B: Chem., **36(1–3)** (1996) 274–277. https://doi.org/10.1016/S0925-4005(97)80081-0

3. Fadeev GI, Kalyakin AS, Somov SI, Electrode potentials of electrochemical cells with oxide-conducting solid electrolyte in chemically nonequilibrium gas mixtures, Russ. J. Electrochem., **45** (2009) 429–433. https://doi.org/10.1134/S1023193509040119

4. Volkov A, Neimin A, Sosnovsky V, Study of durability of the solid electrolyte electrochemical sensors with etalon electrodes of the Me-Me_xO_y type at measuring of the oxygen concentration of the gaseous media (Issledovaniye dolgovechnosti tverdoelektrolitnykh electrokhimicheskikh datchikov s etalonnymi electrodami tipa Me-Me_xO_y pri izmerenii kislorodsoderzhaniya gazovykh sred), Zavodskaya laboratoriya, **48** (1982) 6–8.

5. Zhuiykov S, Miura N. Solid-state electrochemical gas sensors for emission control. In: Sorrell CC, Sugihara S, Nowotny J (eds) Materials for energy conversion devices. Cambridge: Woodhead; 2005. pp 303–335.

6. Park CO, Fergus JW, Miura N, Park J, et al., Solid-state electrochemical gas sensors, Ionics, **15** (2009) 261–284. https://doi.org/10.1007/s11581-008-0300-6

7. Zhuiykov S. Electrochemistry of zirconia gas sensors. Boca Raton: CRC Press; 2008. pp. 1–297. https://doi.org/10.1201/9781420047622

8. Shuk P, Bailey E, Guth U, Zirconia Oxygen Sensor for the Process Application: State-of-the-Art, Sens. Transducers, **90** (2008) 174–184. https://doi.org/10.1007/s11581-008-0274-4

9. Yajma T, Koide K, Fukatsi N, Ohashi T, et al., A new hydrogen sensor for molten aluminum, Sens. Actuators B: Chem., **14(1–3)** (1993) 697–699. https://doi.org/10.1016/0925-4005(93)85149-5

10. Sekhar PK, Brosha EL, Mukundan R, Nelson MA, et al., Development and testing of a miniaturized hydrogen safety sensor prototype, Sens. Actuators B: Chem., **148(2)** (2010) 469–477. https://doi.org/10.1016/j.snb.2010.05.031

11. Miura N, Lu G, Yamazoe N, Progress in mixed-potential type devices based on solid electrolyte for sensing redox gases, Solid State Ion., **136–137** (2000) 533–542. https://doi.org/10.1016/S0167-2738(00)00411-2

12. Lalauze R, Visconte E, Montanaro L, Pijolat C, A new type of mixed potential sensor using a thick film of beta alumina, Sens. Actuators B: Chem., **13(1–3)** (1993) 241–243. https://doi.org/10.1016/0925-4005(93)85371-G

13. Guillet N, Lalauze R, Pijolat C, Oxygen and carbon monoxide role on the electrical response of a non-Nernstian potentiometric gas sensor; proposition of a model, Sens. Actuators B: Chem., **98(2–3)** (2004) 130–139. https://doi.org/10.1016/j.snb.2003.10.001

14. Morata A, Viricelle JP, Tarancón A, Dezanneau G, et al., Development and characterization of a screen-printed mixed potential gas sensor, Sens. Actuators B: Chem., **130(1)** (2008) 561–566. https://doi.org/10.1016/j.snb.2007.09.086

15. Chevallier L, Di Bartolomeo E, Grilli ML, Mainas M, et al., Non-Nernstian planar sensors based on YSZ with a Nb_2O_5 electrode, Sens. Actuators B: Chem., **129(2)** (2008) 591–598. https://doi.org/10.1016/j.snb.2007.09.037

16. Park CO, Akbar SA, Weppner W, Ceramic electrolytes and electrochemical sensors, J Mater Sci., **38** (2003) 4639–4660. https://doi.org/10.1023/A:1027454414224

17. Katahiraa K, Matsumotoa H, Iwaharaa H, Koidea K, et al., A solid electrolyte hydrogen sensor with an electrochemically-supplied hydrogen standard, Sens. Actuators B: Chem., **73(2–3)** (2001) 130–134. https://doi.org/10.1016/S0925-4005(00)00672-9

18. Xia ChY, Lu XCh, Yan Y, Wang T, et al., Improved performances of oxygen potentiometric sensor by electrochemical activation, J Solid State Electrochem., **16** (2012) 2523–2532. https://doi.org/10.1007/s10008-011-1556-8

19. Pasierb P, Rekas M, Solid-state potentiometric gas sensors – current status and future trends, J Solid State Electrochem., **13** (2009) 3–25. https://doi.org/10.1007/s10008-008-0556-9

20. Möbius H-H, Hartung R, Solid-state potentiometric gas sensors – a supplement, J Solid State Electrochem., **14** (2010) 669–673. https://doi.org/10.1007/s10008-009-0839-9

21. Pasierb P, Rekas M, Solid-state potentiometric gas sensors – current status and future trends, J Solid State Electrochem., **13** (2009) 3–25. https://doi.org/10.1007/s10008-008-0556-9

22. Maskell WC, Steele BCH, Solid state potentiometric oxygen gas sensors, J. Appl. Electrochemistry, **16** (1984) 475–489. https://doi.org/10.1007/BF01006843

23. Iwahara H, Uchida H, Ogaki K, Nagato H, Nernstian hydrogen sensor using $BaCeO_3$-based, proton-conducting ceramics operative at 200–900 °C, Journal of the Electrochemical Society, **138** (1991) 295–299. https://doi.org/10.1149/1.2085558

24. Chao Y, Yao S, Buttner WJ, Stetter JR, Amperometric sensor for selective and stable hydrogen measurement, Sens. Actuators B: Chem., **106(2)** (2005) 784–790. https://doi.org/10.1016/j.snb.2004.09.042

25. Lu X, Wu Sh., Wang L., Su Zh., Solid-state amperometric hydrogen sensor based on polymer electrolyte membrane fuel cell, Sens. Actuator B: Chem., **107(2)** (2005) 812–817. https://doi.org/10.1016/j.snb.2004.12.022

26. Tan Y, Tan TC, Sensing behaviour of an amperometric hydrogen sensor, J. Electrochem. Soc., **142** (1995) 1923–1928. https://doi.org/10.1149/1.2044215

27. Sakthivel M, Weppner W, A portable limiting current solid-state electrochemical diffusion hole type hydrogen sensor device for biomass fuel reactors: engineering aspect, Int. J. Hydrogen Energy, **33(2)** (2008) 905–911. https://doi.org/10.1016/j.ijhydene.2007.10.048

28. Kalyakin AS, Volkov AN, Meshcherskikh AN, Dunyushkina LA, Dual chamber YSZ-based sensor for simultaneous measurement of methane and water vapor concentrations in $CH_4 + H_2O + N_2$ gas mixtures, J. Solid State Electrochem., **26** (2022) 739–747. https://doi.org/10.1007/s10008-022-05116-y

29. Medvedev D, Kalyakin A, Volkov A, Demin A, et al., Electrochemical moisture analysis by combining oxygen- and proton-conducting ceramic electrolytes, Electrochem. commun., **76** (2017) 55–58. https://doi.org/10.1016/j.elecom.2017.01.003

30. Taniguchi N, Kuroha T, Nishimura C, Iijima K, Characteristics of novel $BaZr_{0.4}Ce_{0.4}In_{0.2}O_3$ proton conducting ceramics and their application to hydrogen sensors, Solid State Ion., **176(39–40)** (2005) 2979–2983. https://doi.org/10.1016/j.ssi.2005.09.035

31. Tan Y, Tan TC, Sensing behaviour of an amperometric hydrogen sensor, J. Electrochem. Soc., **142(6)** (1995) 1923–1928. https://doi.org/10.1149/1.2044215

32. Bao J, Okuyama Y, Shi Z, Ohno H, et al., Properties of Electrical Conductivity in Y-Doped $CaZrO_3$, Mater. Trans., **53(5)** (2012) 973-979. https://doi.org/10.2320/matertrans.m2012017

33. Goppel W, Reinhardt G, Rasch M, Trends in development of solid state ampermetric and potentiometric high temperature sensors, Solid State Ion., **136–137** (2000) 519–531. https://doi.org/10.1016/S0167-2738(00)00410-0

34. Dubbe A, Fundamentals of solid state ionic micro gas sensors, Sens. Actuators B: Chem., **88(2)** (2003) 138–148. https://doi.org/10.1016/S0925-4005(02)00317-9

35. Somov SI, Reinhardt G, Guth U, Göpel W, Tubular amperometric high-temperature sensors: simultaneous determination of oxygen, nitrogen oxides and combustible

components, Sens. Actuators B: Chem., **65(1–3)** (2000) 68–69. https://doi.org/10.1016/S0925-4005(99)00341-X

36. Usui T, Asada A, Nakazawa M, Osanai H, Gas Polarographic oxygen sensor using an oxygen/Zirconia electrolyte, J. Electrochem. Soc., **136** (1989) 534–542. https://doi.org/10.1149/1.2096676